Chapter 4

Interrogation of the Bell-Evans-Polanyi Principle: Investigation of the Bond Dissociation Enthalpies Correlated with Hydrogen Atom Transfer Rate Constants

4.1 Introduction

The Bell-Evans-Polanyi (BEP) principle is a conceptual framework that states, for two closely related reactions, the difference in activation energy is proportional to the difference in their enthalpy of reaction.[44,45,149]

This is commonly expressed as the linear free energy relationship (LFER): $E_a = E_0 + \alpha\Delta H$ (Equation 1.1). Initially, the BEP principle was used as a simple model to explain the Brønsted catalysis law, which states that the stronger an acid is, the faster the catalyzed reaction will proceed.[150] A key assumption is made for the BEP principle: the position of the TS along the reaction coordinate is the same for all reactions. The relationship can be described schematically: the more stable the product, the lower the reaction barrier, as seen in Figure 4.1.

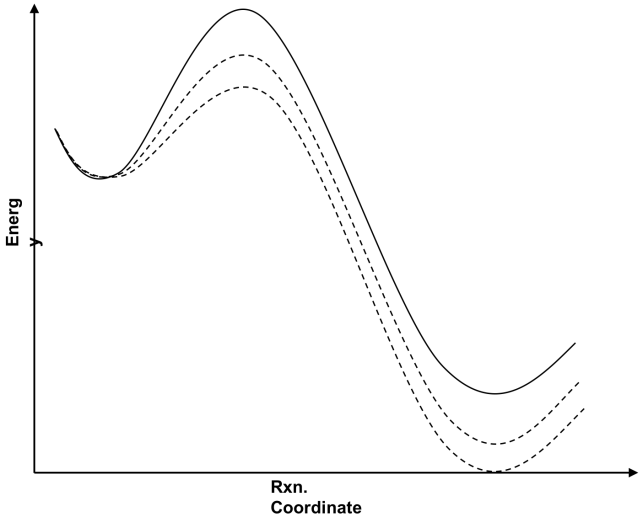

Figure 4.1: Energy profiles for a series of related exothermic reactions illustrating the Bell-Evans-Polanyi principle.

A modern utilization of the BEP principle is to estimate rate constants of related reactions. This is a desirable, because as system size increases, ab initio computational modelling becomes computationally challenging, or even infeasible due to the exponential scaling of computational cost with system size. Therefore, the main purpose of LFERs is to apply previous

knowledge to new systems and help develop insights. For example, much of our groups' work focuses on studying simple protein models. By thoroughly investigating small systems with ab initio approaches, it is possible to extrapolate the fundamental concepts to large-scale systems. Furthermore, if one can establish that there exists a LFER between activation energy and bond strength for a specific model, then the difference in bond dissociation enthalpy (BDE) can be used to estimated HAT reaction rates in a large-scale protein system.

In application of the BEP principle in HAT reactions, plots of the logarithm of the rate constant (k_H) against BDEs are commonly used: $\log(k_{\mathrm{H}}) = \alpha\Delta H + constant$. For HAT reactions involving abstraction by CumO$^{\bullet}$, the enthalpy of reaction (ΔH) is directly related to the strength of the breaking bond: $\Delta H = \mathrm{BDE(C{-}H)} - \mathrm{BDE(CumO{-}H)}$. If the relationship holds for a series of related HAT reactions, then BDEs should correlate with the activation energy. It would then stand that an increase in bond strength represents a destabilization in the TS complex, and thus a decrease in reaction rate. This concept is also important for the work in Chapter 5, where the interaction of non-redox active metal cations results in an increase in effective bond strength, and decrease in rate constant. It is also important to note that if the BEP principle breaks down for reactions that appear related, then additional physico-chemical factors, such as non-covalent binding (*viz.* Chapter 3), or stereo-electronics may be influencing the reaction barrier.

An interesting application of the BEP principle is the work of Pratt et al.[151], in which the free radical oxidation of unsaturated lipids was examined. They studied the correlation of theoretically determined allylic

or benzylic C-H and C−OO$^\bullet$ bond strengths with experimentally-measured HAT rate constants and O_2 addition rate constants, respectively. BEP plots ($\log k$ vs. BDE) for a large range of polyunsaturated fatty acid models show good correlation for C−OO$^\bullet$ bonds examined, and reasonable correlation for C−H bonds. This demonstrates that BDEs may directly impact the reaction barrier height, in line with the BEP principle. Additionally, these results provide the important ability of predicting rate constants for HAT and oxygen addition reactions related to unsaturated lipid models, by means of calculating BDEs. Another area of research in which the BEP principle is often applied is heterogenous catalysis.[152]

There is a significant gap in the literature on the BEP principle: there are no criteria for how broadly the BEP principle can be utilized. In fact, the theoretical validity of the BEP relationship has come into question, and a call has been made to theoreticians for a detailed analysis of the BEP principle.[153] In this work, I explore this issue. In order to achieve this, I have studied HAT reactions involving the abstraction of C-H bonds by CumO$^\bullet$ under the same experimental conditions, for which many rate constants have been published.[46,129,130,132,133,154–156] Additional unpublished rate constants have been provided by our experimental colleagues in Rome. The above studies, as well as many others, have used CumO$^\bullet$ and the closely related *t*-butoxyl radical (t−BuO$^\bullet$) as models for reactive oxygen-centred radicals in studying oxidative damage of biomaterials,[157–159] as well as in studying the mechanism and efficiency of antioxidants.[160–164] Using these radicals to study biomolecular oxidation has an important caveat: The fundamental chemistry of these radicals is less well understood than often assumed.[36,37,165]

The BDE[v] of CumO−H is 106.7 kcal mol^{-1}, a value that is larger than all the C−H bonds studied herein. Therefore, these reactions are all exothermic on the order of 5–32 kcal mol^{-1}. The transition states can then be described as early, by the Hammond Postulate, and the BEP α values should all be less than 0.5.[166] Now, if the BEP principle holds as a LFER, the substrates should be considered as if the BDEs were controlled by substituent effects. For example, if one considers methane as the reference C−H bond model, the BDE of toluene should reflect the effect of replacing one hydrogen with a phenyl group. This is also the basis for schemes that utilize group additivity to predict molecular heats of formation.[143]

Considering this group additivity-like approach, I have hypothesized that there should exist two general BEP relations for C-H bond: one in which the incipient radical is delocalized into a π-system (benzylic or allylic), and one in which the remaining alkyl radicals are largely localized. Plotting the experimental rate constants against literature BDEs (Figure 4.2) there appears to be evidence for the two BEP relations.

There is a considerable amount of scatter in Figure 4.2, which may be due to differences in experimental procedures. BDEs are measurable using a large number of different experimental techniques, and a great deal of data exists in the literature. Much of this data has conveniently been compiled in the *de facto* reference for BDEs: the *CRC Handbook of Bond Dissociation Enthalpies*.[167] However, caution must be taken with experimentally determined BDEs, as not all experimental methods give reliable data. For example, BDEs from the Bordwell[168] thermochemical cycle are

[v] Calculated using the ROCBS-QB3 composite method, *vide infra*.

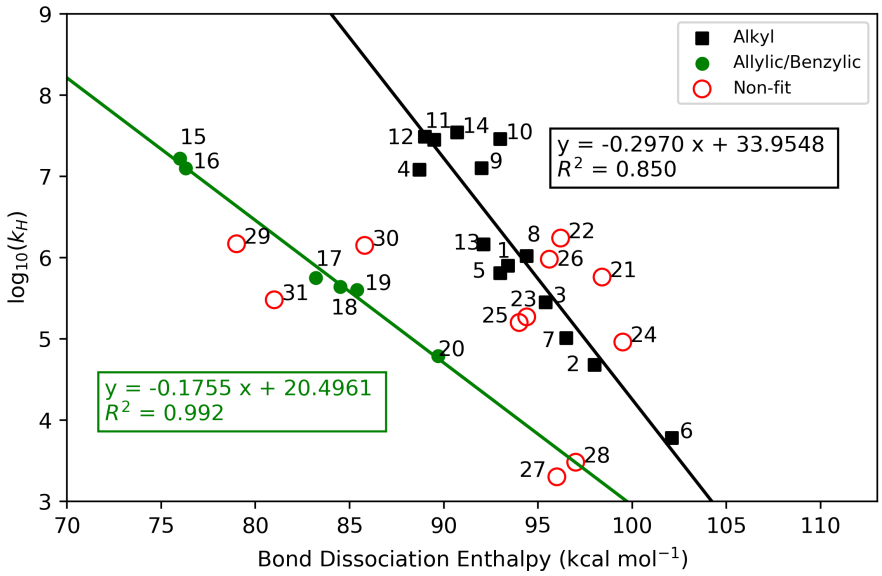

1	1,4-diazobicyclo[2.2.2]octane	2	2,2-dimethylbutane
3	2,2-dimethylbutane	4	Benzaldehyde
5	Diethyl ether	6	Dimethyl sulfoxide
7	Dioxane	8	Hexamethylphosphoramide
9	Morpholine	10	Piperazine
11	Piperidine	12	Pyrroldiine
13	Tetrahydrofuran	14	Triethylamine
15	1,4-cyclohexadiene	16	9,10-dihydroanthracene
17	Cumene	18	Diphenylmethane
19	Ethylbenzen	20	Toluene
21	Adamantane (2°)	22	Adamantane (3°)
23	Cycloheptane	24	Cyclohexane
25	Cyclooctane	26	Cyclopentane
27	Acetone	28	Acetonitrile
29	Benzyl alcohol	30	Dibenzyl ether
31	Triphenylmethane		

Figure 4.2: Bell-Evans-Polanyi plot of experimental rate constants (normalized for the number of equivalent hydrogen atoms) for HAT between CumO$^{\bullet}$ and substrates against literature BDEs. BDEs for dimethyl sulfoxide and hexamethylphosphoramide are from Ref. 133, while all other BDEs are from Ref. 167.

possibly unreliable.[133,169] This was demonstrated for the BDE of dimethyl sulfoxide (DMSO), for which the experimentally determined BDE is about 8 kcal mol^{-1}lower than the best computational estimate.[133] Therefore, quantum chemistry is a useful tool for studying BDEs, as it is relatively simple to compute BDEs. An arbitrary X−H bond dissociation enthalpy is given by:

$$\Delta H(BDE) = H(\mathrm{X}^{\bullet}) + H(\mathrm{H}^{\bullet}) - H(\mathrm{X{-}H}) \tag{4.1}$$

where $\Delta H(BDE)$ is the BDE, and the right-hand terms are the enthalpies of the radical product, the hydrogen atom, and the substrate, respectively. By computing the most accurate BDEs possible, we are able to discern if the BEP principle holds for C−H bond hydrogen abstraction by CumO$^{\bullet}$.

DFT-based methods have been shown to give reliable relative BDEs, however, highly correlated wave function based methods are required to predict chemically accurate (sub-kcal mol^{-1}) BDEs.[170–172] For this purpose, we shall use composite quantum chemical procedures. Unfortunately, due to the computational cost of some of these procedures, calculations are often limited to small molecules. Additionally, there is currently no literature that compares the ability of common composite methods to predict accurate BDEs. Therefore, another aim of the work is to determine which composite procedure can be used to calculate accurate BDEs for relatively large molecules.

4.2 Methods

Experimental rate constants were either provided from unpublished results from our colleagues in Rome, or come from literature sources.[46,129,130,132,133,154–156] All rate constants come from laser flash photolysis (LFP) experiments of CumO$^\bullet$ with the substrates of interest. Acetonitrile solvent and ambient conditions (298 K and 1 atm) were used in all cases. For those results that are unpublished, CumO$^\bullet$ is generated by laser pulses at either 266 nm or 355 nm in solutions of excess dicumyl peroxide. Many of the literature results are also from the Bietti group, where the same procedure is used. Other results may have small variations in experimental details, however, all results are well time-resolved.

Observed rate constants (k_{obs}) are generally obtained from 2–8 averaged trials, which are reproducible to within 5%. Transient absorption decay traces of CumO$^\bullet$ monitored at 485 nm are used to determine k_{obs}. The observed rate constant is plotted against concentration of substrate to provide the bimolecular HAT rate constant (k_H) as the slope ($k_{obs} = k_0 + k_H[substrate]$). The CumO$^\bullet$ radical decays unimolecularly through the β-scission of a methyl group, giving acetophenone and a methyl radical, as shown in Scheme 4.1. The unimolecular decay rate constant[173,174] for CumO$^\bullet$(k_0) in acetonitrile is on the order of 6.3 $\times 10^5$ s^{-1} at 298 K.

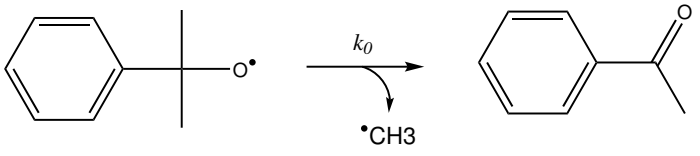

Scheme 4.1: Unimolecular decay of the cumyloxyl radical.

All quantum chemical calculations were performed using the Gaussian 09 software package.[104] Several composite quantum chemical methods that are implemented in Gaussian 09 were used in this work: W1BD, CBS-QB3 and the restricted open-shell variant ROCBS-QB3, CBS-APNO, G4 and the MP2 variant G4(MP2). An approach using ROCCSD(T) with locally-dense basis sets[175,176] (LDBS) was also utilized in order to approximate W1BD results. Each of these methods is briefly described below.

4.2.1 Quantum chemical composite procedures

W1BD

The highest-accuracy method used is W1BD, which employs seven different calculations to obtain highly-correlated electronic energies, as well as thermochemically corrected quantities. This method is very computationally expensive, and thus cannot be applied to the larger species of interest in this work. Geometries and thermochemical corrections come from DFT-based B3LYP calculations with nearly complete cc-pVTZ+d basis sets. A frequency scaling factor of 0.985 is used to obtain thermochemical corrections. The electronic energy comes from several additive corrections involving the Brueckner Doubles[84] (BD) variation of coupled cluster and large basis sets extrapolated to the complete basis set limit. Corrections for core-electron correlation and relativistic contributions are computed using an uncontracted variant of the cc-pVTZ+2df basis sets, known as MTsmall.[177]

LDBS approach

Locally-dense basis sets have been used in the past to calculated BDEs

for relatively large molecules.[175,176,178] The principle behind LDBS is to use large basis sets to treat the atomic centres that are directly involved in the chemistry taking place, and use progressively smaller basis sets for "remote" portions of the molecule, thus taking advantage of error cancellation. We chose a method that best approximates W1BD results for a small subset of molecules. The scheme utilized herein involves geometry optimization and scaled frequency calculations from DFT-based B3LYP/cc-pVTZ+d, as used in the W1BD procedure. Single-point energy calculations are then performed using ROCCSD(T) and an LDBS partitioning scheme we denote as pc-3/3/2/1, demonstrated in Scheme 4.2, using the polarization consistent basis sets.[59]

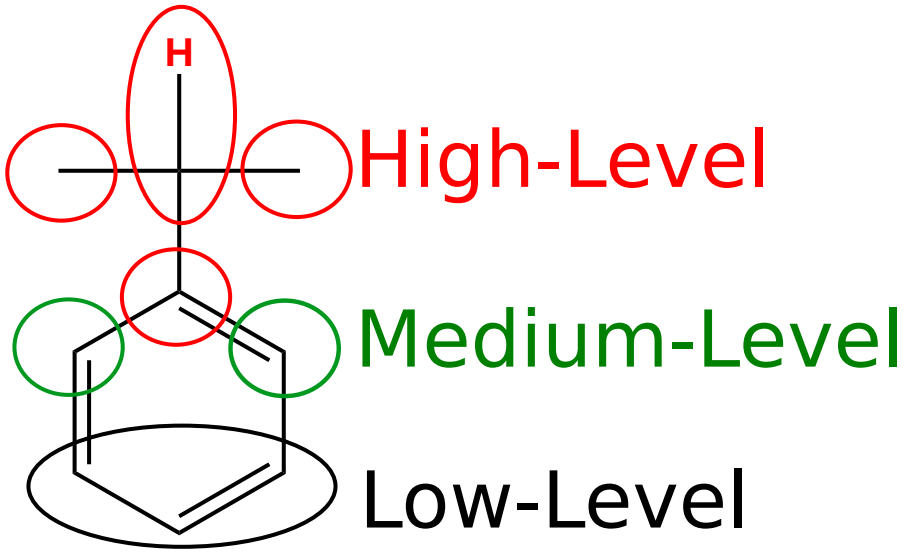

Scheme 4.2: Locally-dense basis set partitioning used in the calculation of BDEs. The scheme is referred to as pc-3/3/2/1, where for the shown cumene molecule, the centre of C−H cleavage and the immediately adjacent groups are treated with high-level pc-3 basis sets. The next groups are treated with medium-level pc-2 basis sets, and all other atoms/groups are treated with low-level pc-1 basis sets.

CBS methods

The Complete Basis Set (CBS) methods of Petersson and colleagues[81–83,179] are widely used because of the relatively low computational cost (compared to other composite procedures), and well-established accuracy.[180,181] CBS-QB3[81,82] utilizes DFT-based B3LYP optimization and scaled frequencies (factor = 0.990) with modified triple-zeta Pople style basis sets. Electronic energies are obtained by extrapolation of medium basis set CCSD(T) and MP4SDQ. Small empirical corrections are added to achieve more accurate results compared to the parametrization sets.[182] ROCBS-QB3 is a similar

procedure to CBS-QB3, except spin-restricted wave functions are used in place of unrestricted wave functions. This is done to eliminate spin contamination, and the use of a restricted open-shell definition has been shown to produce more accurate BDEs.[170] The (RO)CBS-QB3 methods have been implemented for the first, second, and third periods of elements.

Atomic pair natural orbital (APNO) expansions are a method used for averaging over multiple Slater determinants. The use of APNOs allows for small basis set extrapolation of higher order correlation energies to converge more rapidly to the complete basis set limit. This approach is used in the CBS-APNO method.[83] Geometries and scaled frequencies (factor = 0.989) are obtained at the QCISD/6-311G(d,p) level of theory. Similar to CBS-QB3, the extrapolation of moderate basis set MP4SDQ and QCISD(T) results gives the electronic energy. An empirical correction is also used in CBS-APNO. Although CBS-APNO is more accurate, the expansion of APNOs makes CBS-APNO more computationally demanding than CBS-QB3. As a result, CBS-APNO has only been implemented for first and second row periods, and is thus less commonly used in the literature.

Gn methods

The Gaussian$-n$ (Gn) series of methods originates from the Pople group,[183] and G4 is the fourth generation. G4 utilizes moderately large basis sets and extrapolation techniques with CCSD(T) calculations to obtain highly correlated electronic energies. G4(MP2) uses MP2 in place of CCSD(T) and is thus less computationally expensive, but also gives a less complete description of electron correlation. Both methods use the B3LYP/6-31(2df,p)

level of theory for optimization and frequency calculations with a frequency scaling factor of 0.9854. G4 results have been described as generally on par with CBS-QB3 results,[180,181] but calculations are more computationally expensive.

4.2.2 Transition state calculations

Calculations were performed to identify the lowest energy TS complex of several reactions between CumO$^{\bullet}$ and organic substrates. In all cases cisoid and transoid conformations were explored. All optimization calculations were performed at the B3LYP-D3(BJ)/6-31+G* level of theory, followed by single-point energy calculations at the LC-ωPBE-D3(BJ)/6-311+G** level of theory. The latter DFT-based method was selected to minimize delocalization error in the TS complex.[100] Transition states were visualized using the Chemcraft program[184] to confirm a single imaginary frequency connecting reactants to products. In some cases, a small secondary imaginary frequency was observed, indicating a TS complex that is not fully optimized. Necessary steps were taken to re-optimize the structures and eliminate the small imaginary frequencies, however, this was not always successful. Nonetheless, I am confident the structures reported herein sufficiently represent the true TS complex geometries and relative energies. Results from structures that are not fully optimized are indicated appropriately as such.

4.3 Comparison of composite method for the prediction of BDEs

In order to determine the best method for BEP principle analysis, and to investigate which is the most efficient yet accurate composite method, the BDEs of 50 species have been calculated. This set of species contains a wide variety of chemical functionalities with BDEs ranging from 75–113 kcal mol^{-1}, thus this set may be described as a comprehensive test of these methods for C-H BDEs. Given that W1BD is the most accurate method used, these results have been used for comparison to other composite methods. However, BDEs for only 33 out of the 50 species studied were able to be calculated using W1BD due to computational cost restrictions: hard disk capacity was insufficient for large systems. Therefore, literature BDEs from Luo [167] for the 49 species that have literature values in the set are also used for comparison. The literature and calculated BDEs are listed in Table 4.1.

Table 4.1: Bond dissociation enthalpies of the species used to investigate the accuracy of composite methods. All values are in kcal mol^{-1}. Statistics are listed at the bottom of the table

Molecule	Lit.[167]	W1BD	LDBS	CBS-QB3	ROCBS-QB3	CBS-APNO	G4	G4(MP2)
1,3-pentadiene	83.0	82.9	82.2	80.9	81.7	81.8	81.6	82.1
1,4-diazabicyclo[2.2.2]-octane	93.4		98.9	98.9	98.8	98.5	96.7	95.6
1,4-pentadiene	76.6	76.2	76.0	74.2	75.0	75.2	75.1	75.7
2,2-dimethylbutane	98.0	99.3	99.1	99.4	99.3	99.7	97.5	96.7
2,3-dimethylbutane	95.4	97.8	97.7	97.9	97.8	98.0	96.2	95.5
2-methylbutane	95.8	97.3	97.2	97.3	97.1	97.3	95.9	95.5
Acetaldehyde	94.3	95.9	95.3	95.3	95.7	95.5	94.9	94.8
Acetone	96.0	96.9	96.4	96.2	96.7	97.1	95.4	95.0

Molecule	Lit.[167]	W1BD	LDBS	CBS-QB3	ROCBS-QB3	CBS-APNO	G4	G4(MP2)
Acetonitrile	97.0	96.9	96.6	96.2	96.6	96.5	96.3	96.3
Adamantane (2°)	98.4		100.9	100.5	100.4	100.9	97.8	96.3
Adamantane (3°)	96.2		100.3	99.9	99.9	100.3		95.7
Benzaldehyde	88.7		90.9	91.5	91.4	91.0	89.3	88.2
Benzene	112.9	113.1	112.7	115.4	113.0			113.0
Benzyl Alcohol	79.0		84.4	84.3	83.2	83.9	83.4	83.6
Cumene	83.2		87.9	87.9	86.9		86.9	86.7
Cycloheptane	94.0		96.0	96.0	95.8	96.1	93.9	92.9
Cyclohexadiene	76.0	76.3	76.2	74.3	75.0		75.2	75.5
Cyclohexane	99.5	99.2	99.1	99.4	99.3	99.6	97.5	96.8
Cyclooctane	94.4		92.6	92.6	92.4	92.8	90.2	89.1
Cyclopentane	95.6	96.3	96.1	96.5	96.3	96.6	95.6	95.0
Cyclopropane	106.3	109.0	108.5	109.3	109.2	109.5	108.2	108.0
Dibenzyl ether	85.8		83.6	84.3	82.7			79.6

Molecule	Lit.[167]	W1BD	LDBS	CBS-QB3	ROCBS-QB3	CBS-APNO	G4	G4(MP2)
Diethyl ether	93.0	95.3	95.1	95.6	95.5	95.4	93.8	93.1
Dihydroanthracene	76.3		80.4	80.9	78.1			79.9
Dimethylamine	94.2	92.6	92.4	92.9	92.8	92.7	92.0	91.9
Dimethylsulfoxide	94.0	102.0	101.7	102.3	102.3		100.9	100.6
Dioxane	96.5	97.3	97.3	97.7	97.6	97.4	95.7	94.9
Diphenylmethane	84.5		84.1	85.3	82.8			84.5
Ethane	100.5	101.3	99.3	101.7	101.5	101.8	100.7	100.7
Ethylbenzene	85.4		88.3	88.6	87.6	89.3	87.6	87.7
Ethylene	110.9	110.8	110.3	110.6	110.9	111.1	109.9	110.2
Fluorene	82.0		82.4	83.6	81.9			81.2
Formaldehyde	88.0	88.6	88.0	89.1	88.9	88.2	88.2	87.9
Hexamethyl-phosphoramide			93.8	94.1	93.9			88.5
Indene	83.0		80.6	80.4	80.1	81.2	79.0	78.3

Molecule	Lit.[167]	W1BD	LDBS	CBS-QB3	ROCBS-QB3	CBS-APNO	G4	G4(MP2)
Methane	105.0	105.0	104.4	105.4	105.2	105.4	104.5	104.6
Methanol	96.1	96.4	96.0	96.9	96.8	96.6	96.0	95.8
Methylamine	93.9	93.1	92.8	93.4	93.3	93.3	92.7	92.8
Morpholine	92.0		93.4	93.4	93.3	93.3	91.8	91.1
N,N-dimethylacetamide (acetyl)	91.4	99.6	99.4	99.5	99.5	100.1	97.6	96.8
Piperazine	93.0	93.4	93.5	93.6	93.5	93.4	91.9	91.2
Piperidine	89.5	92.1	92.2	92.3	92.2	92.1	90.7	90.0
Propane	100.9	101.6	101.3	102.0	101.8	102.1	100.7	100.4
Pyrrolidine	89.0	90.8	90.6	90.8	90.7	90.7	89.5	89.0
Tetrahydro-2H-pyran	96.0	96.3	96.2	96.6	96.5	96.3	94.7	93.9
Tetrahydrofuran	92.1	93.7	93.3	93.9	93.8	93.6	92.2	91.6

Molecule	Lit.[167]	W1BD	LDBS	CBS-QB3	ROCBS-QB3	CBS-APNO	G4	G4(MP2)
Toluene	89.7	90.5	90.1	90.6	89.7	91.9	89.8	90.2
Trichloromethane	93.8	93.5	93.4	93.8	93.7		92.4	92.0
Triethylamine	90.7		91.4	91.3	91.2	91.4	89.4	88.4
Trifluormethane	106.4	107.2	106.6	107.4	107.4	106.8	105.8	105.0
Statistics	Lit.	W1BD	LDBS	CBS-QB3	ROCBS-QB3	CBS-APNO	G4	G4(MP2)
Number of BDEs (N)	49	33	50	50	50	40	43	50
MAE (Lit.)		0.82	1.60	1.88	1.64	1.35	1.21	1.57
Max. Error		1.59	2.41	2.63	3.15	1.85	4.19	6.23
Min. Error		-8.22	-8.04	-8.26	-8.25	-8.74	-6.86	-6.58
MAE (W1BD)			0.22	0.32	0.18	0.20	0.70	0.88
Max. Error			2.00	2.01	1.26	1.08	2.05	2.84
Min. Error			-0.09	-2.37	-0.35	-1.39	0.37	0.02

Mean absolute error (MAE) is used to assess the quality of computational methods, where errors are calculated with respect to benchmark values for a given data set.[185] The MAE is calculated as

$$\mathrm{MAE} = \frac{1}{N} \sum |E_{ref} - E_{calc}| \tag{4.2}$$

where, for a set of N reference values, the MAE is the average of the mean differences of the reference energy (E_{ref}) and the calculated value (E_{calc}). The MAE with respect to W1BD and literature shall be reported herein as "$\mathrm{MAE_{W1BD}}$ ($\mathrm{MAE_{Lit.}}$)". An additional semi-quantitative metric which I used to evaluate the accuracy of composite procedures to reproduce experimental results is a bar chart that summarizes the number of deviations from literature within given error ranges. This bar chart is reported in Figure 4.3. Note that calculations for some species with some methods failed to converge, thus number of BDEs out of 49 are also shown in Figure 4.3. Also, an alternative method that I shall utilize for reporting these data is through the use of one-to-one plots, in which BDEs from two methods are directly compared. An ideal plot should have a slope = 1 and y-intercept = 0.

Comparing W1BD results to literature, the MAE is 0.82 kcal $\mathrm{mol^{-1}}$, and the majority of the data match to within 1–2 kcal $\mathrm{mol^{-1}}$of literature. Thus, W1BD is largely consistent with the literature values. Additionally, the one-to-one plots comparing W1BD to literature in Figure 4.4 show reasonable agreement with slope of 0.98 and a y-intercept of 2.35. There are, however, two notable outliers: DMSO[vi] and *N,N*-dimethylacetamide, for

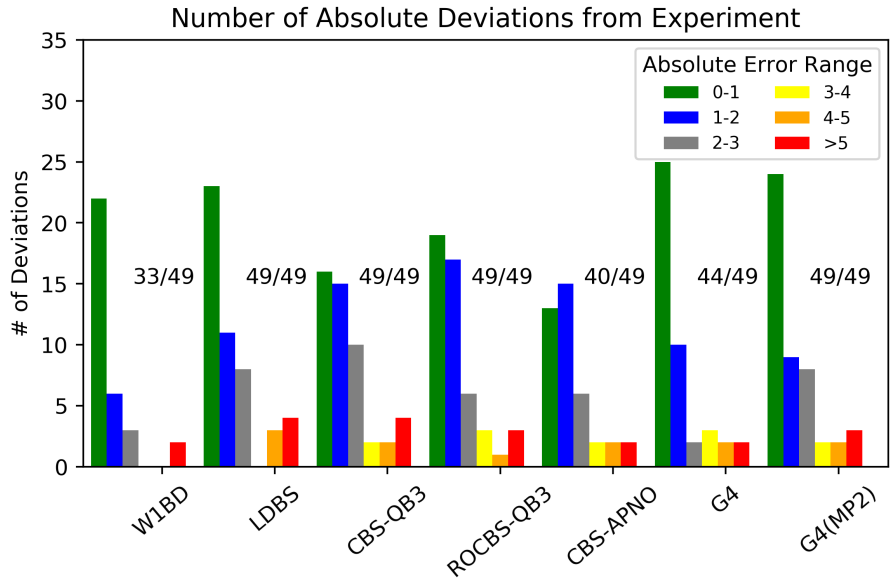

Figure 4.3: Summary of deviations of BDEs from literature or composite quantum chemical methods. Errors are units of kcal $mol^{-1}$and are relative to Ref. 167. Numbers out of 49 represent the total number of data points that were computed for the given method.

which experiment underestimates the BDEs by -8.0 and -8.2 kcal mol^{-1}, respectively. DMSO and *N,N*-dimethylacetamide are consistently outliers amongst all composite methods, suggesting the literature BDEs are incorrect.

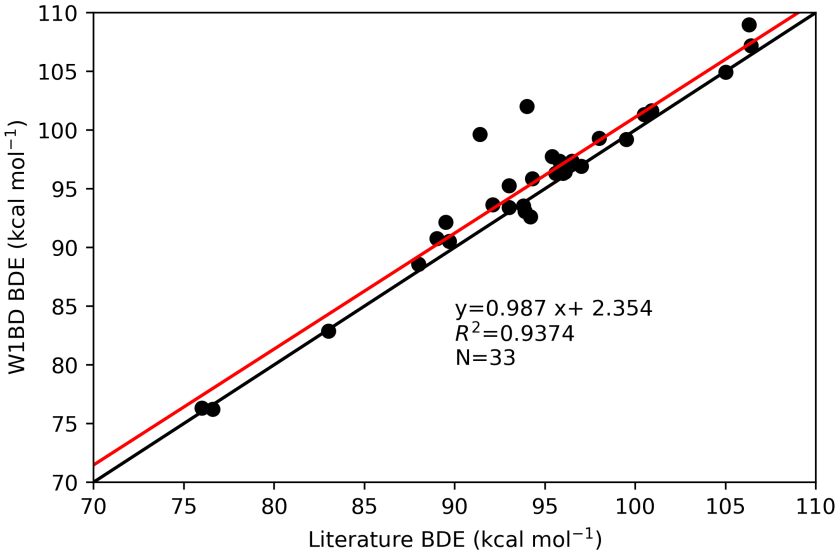

Figure 4.4: One-to-one plot of BDEs from literature[167] and as calculated by the W1BD composite method. The red line represents the least squares line of best fit, while black line represents a perfect one-to-one correlation.

The method that gives the best combined agreement with W1BD and literature is ROCBS-QB3 with an MAE = 0.18 (1.64) kcal mol^{-1}. It is also apparent, from the one-to-one plots in Figure 4.5, that ROCBS-QB3 matches well with literature and experiment. In comparison, CBS-QB3 has an MAE = 0.32 (1.88) kcal mol^{-1}, while CBS-APNO has an MAE = 0.20 (1.40) kcal

[vi] The experimental BDE for dimethyl sulfoxide was previously identified as being inaccurate by Salamone et al.[133]

mol^{-1}. The LDBS approach also performs well with an MAE = 0.22 (1.60) kcal mol^{-1}. The G4 method deviates from the W1BD reference by about 0.5 kcal mol^{-1} more, however, it appears to give reasonable agreement with experimental results (MAE = 0.70 (1.21) mol). The use of the MP2 variant of G4 gives somewhat questionable results, with an MAE of 0.88 (1.60) kcal mol^{-1}, as well as a large outlier of 6.2 kcal mol^{-1} that is not present in the other data from composite methods. One-to-one plots of all other methods are presented in Appendix B.

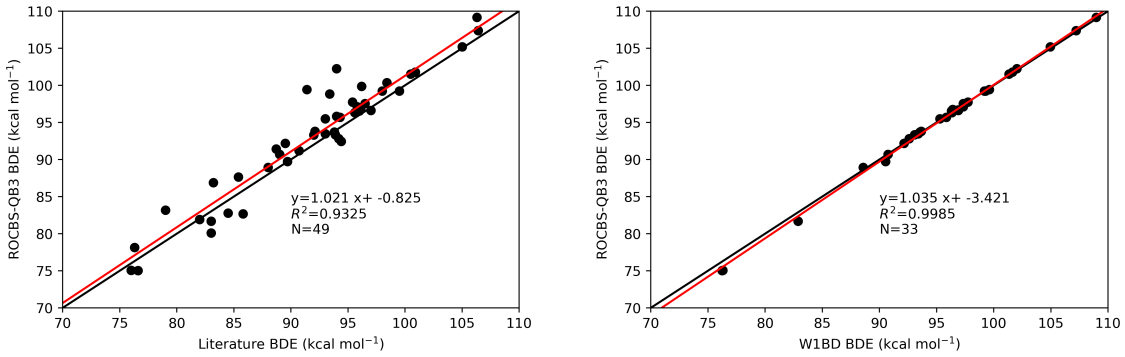

Figure 4.5: One-to-one plot comparing calculated BDEs calculated by the ROCBS-QB3 to reference literature[167] and W1BD BDE values, respectively. The red line represents the least squares line of best fit, while black line represents a perfect one-to-one correlation.

In summary, ROCBS-QB3 performs best for the calculation of C−H BDEs while G4(MP2) performs worst. Given these data, and considering the relative computational cost, I recommend the ROCBS-QB3 for the calculation of accurate BDEs, particularly for large molecules for which more expensive computational methods are not possible. Importantly, we can now confidently continue investigating the BEP relationships using reliably

calculated BDE data from the ROCBS-QB3 method. Furthermore, these results can be extended to even larger systems as the ROCBS-QB3 approach is one of the least computationally-expensive composite methods. For example, calculations on the cyclohexane molecule, which take about 20 minutes using ROCBS-QB3 on SGI Altix compute nodes with 6 processors and 8 GB RAM, while G4 takes approximately 27 times longer, the LDBS approach takes about 500 times longer, and W1BD takes about 1100 times longer.

4.4 Analysis of the Bell-Evans-Polanyi principle

We turn now to the application of accurate BDEs to the BEP principle. Experimental HAT rate constants have been collected for 32 reactions involving CumO$^{\bullet}$ and organic substrates. The BEP plot of the logarithm of rate constants divided by the number of equivalent H atoms (i.e., normalized) against BDEs is shown in Figure 4.6.

As with the experimental results in Figure 4.2, there clearly exists two distinct regions in Figure 4.6. This is congruent with our initial hypothesis that there should exist two linear relations: one for allylic/benzylic C-H bonds, and another for alkyl C-H bonds. However, there remains a considerable amount of scatter in the data, thus correlation of the expected BEP relations is poor. For the allylic/benzylic series of C-H BDEs which result in a radical which is delocalized, the correlation coefficient is 0.89. This result is consistent with work of Pratt et al.,[151] which found a BEP plot correlation coefficient of 0.82 for the abstraction of C-H bonds from models for unsaturated fatty acids. Most of the rate constants used in the work of

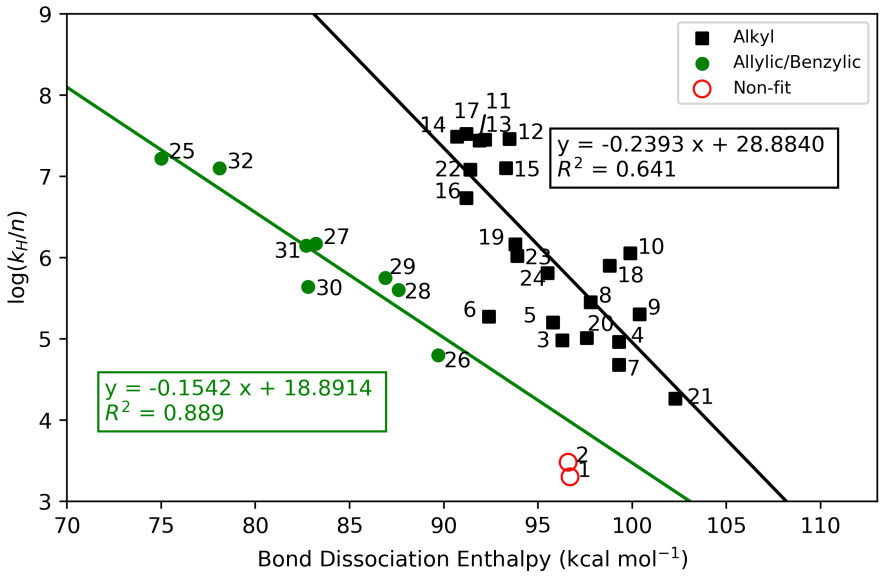

1	Acetone	2	Acetonitrile
3	Cyclopentane	4	Cyclohexane
5	Cycloheptane	6	Cyclooctane
7	2,2-dimethylbutane	8	2,3-dimethylbutane
9	Adamantane (2°)	10	Adamantane (3°)
11	Diethyl amine	12	Piperazine
13	Piperidine	14	Pyrrolidine
15	Morpholine	16	Propylamine
17	Triethylamine	18	1,4-diazobicyclo[2.2.2]octane
19	Tetrahydrofuran	20	Dioxane
21	Dimethyl sulfoxide	22	Benzaldehyde
23	Hexamethylphosphoramide	24	Diethyl ether
25	1,4-cyclohexadiene	26	Toluene
27	Benzyl alcohol	28	Ethylbenzene
29	Cumene	30	Diphenylmethane
31	Dibenzyl ether	32	9,10-dihydroanthracene

Figure 4.6: Bell-Evans-Polanyi plot of experimental rate constants (normalized for the number of equivalent hydrogen atoms) for HAT between CumO$^{\bullet}$ and substrates against BDEs calculated using the ROCBS-QB3 method.. Acetone and acetonitrile are note included in fitting as the experimental rate constants are approximate.

Pratt et al. are for the abstraction of C−H by peroxyl radicals, which were obtained through an experimental method that gives estimated HAT rate constants with large associated errors. Thus, they suggested that the degree of scatter is associated with experimental errors. The same however cannot be said for the rate constants associated with this work. Therefore, there must be additional physico-chemical factors at play.

The alkyl C-H BDEs show very weak correlation with CumO$^{\bullet}$ HAT rate constants, with a correlation coefficient of 0.63. One possibility is that applying the BEP principle to such a large grouping of substrates is inappropriate. Thus, I have re-plotted this data in Figure 4.7, breaking the data into several smaller chemical groupings: cyclic alkanes, other alkanes, tertiary amines (Tert. Amines), hydrogen bond donating (H-Bond Donors) species, and other C−H bonds with heteroatom neighbours (Het. Neighbours). Doing so appears to reveal one well-correlated trend for C−H bonds with heteroatom neighbours ($R^2 = 0.96$). There are two data points for the tertiary amines, thus the points should not be fit to a line, however it is unclear why they do not fit into the other heteratomic neighbours trend. The cyclic alkanes are poorly correlated ($R^2 = 0.73$). Extremely poor correlation is observed for both the hydrogen bond donating species ($R^2 = 0.02$) and other alkanes ($R^2 = 0.01$). There are no evident reasons on the basis of group-additivity based arguments that explain the poor correlations observed. Thus, the lack of simple relationships is perhaps evidence against the validity of the BEP principle. However, before making any conclusions, we must consider if there are any explanations that arise from examining the transition state structures.

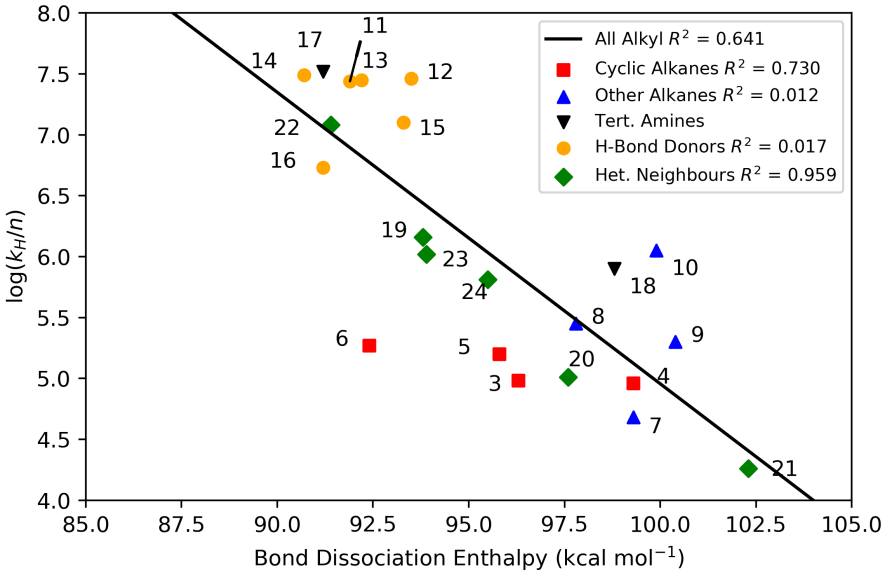

3	Cyclopentane	4	Cyclohexane
5	Cycloheptane	6	Cyclooctane
7	2,2-dimethylbutane	8	2,3-dimethylbutane
9	Adamantane (2°)	10	Adamantane (3°)
11	Diethyl amine	12	Piperazine
13	Piperidine	14	Pyrrolidine
15	Morpholine	16	Propylamine
17	Triethylamine	18	1,4-diazobicyclo[2.2.2]octane
19	Tetrahydrofuran	20	Dioxane
21	Dimethyl sulfoxide	22	Benzaldehyde
23	Hexamethylphosphoramide	24	Diethyl ether

Figure 4.7: Further breakdown of Bell-Evans-Polanyi plot of experimental rate constants (normalized for the number of equivalent hydrogen atoms) for HAT between CumO$^{\bullet}$ and substrates.

4.5 Transition state analysis

In order to determine if there are any reasons for the breakdown of the BEP principle, I have calculated TS structures for 20 of the reactions at the LC-ωPBE-D3(BJ)/6-311+G(2d,2p)//B3LYP-D3(BJ)/6-31+G* level of theory. The calculated reaction free-energy barrier heights ($\Delta G^{\ddagger}$) are listed in Table 4.2, along with the decomposition into enthalpic and entropic terms: $\Delta G^{\ddagger} = \Delta H^{\ddagger} - T\Delta S^{\ddagger}$.

First, consider some general features associated with the TS complexes listed in Table 4.2. One factor that may lead to deviations from the BEP principle is the possibility for different HAT reaction mechanisms, i.e. direct HAT or PCET. Consider first the reaction of toluene with CumO$^{\bullet}$. As this reaction is similar to the self-exchange reaction of the benzyl-toluene couple as described by DiLabio and Johnson,[26] one might expect the reaction to proceed via PCET. The lowest-energy TS complex has a partially π-stacked conformation with the rings oriented approximately 40° relative to one another. Examination of the SOMO and HOMO reveals no π-π partial bonding interaction, as can be seen in Figure 4.8. The electron density of the SOMO is largely localized on the toluene portion of the complex. This is likely due to the additional non-conjugated carbon centre of CumO$^{\bullet}$, which prevents an additional electron channel for PCET to occur. Therefore, this reaction takes place through direct HAT, as has been previously described.[129] This behaviour is specific to the CumO$^{\bullet}$ radical, thus all the reactions likely also take place through a direct HAT mechanism, and this should not factor into the deviations in the observed BEP principle relationships.

Table 4.2: Reaction barrier heights for reactions of substrates with $CumO^{\bullet}$ calculated in the gas phase at 298 K at the LC-ωPBE-D3(BJ)/6-311+G(2d,2p)//B3LYP-D3(BJ)/6-31+G* level of theory. All values are in units of kcal mol^{-1}. ID numbers match those in Figure 4.6 †TS structure contains small additional imaginary frequency.

ID	Substrate	$\Delta G^{\ddagger}$	$\Delta H^{\ddagger}$	$-T\Delta S^{\ddagger}$
	Non-fit			
1	Acetone	17.6	3.6	14.0
2	Acetonitrile	18.3	6.8	11.5
	Cyclic Alkanes			
3	Cyclopentane†	13.5	0.5	13.0
4	Cyclohexane	11.8	1.2	10.6
6	Cyclooctane†	13.6	-0.5	14.1
	Other Alkanes			
7	2,2-dimethylbutane	11.2	-0.8	12.0
8	2,3-dimethylbutane	11.2	1.1	10.2
9	Adamantane (2°)	12.6	0.6	12.0
10	Adamantane (3°)	10.8	-1.0	11.8
	Tert. Amine and H-Bond Donor			
11	Diethylamine	10.0	-3.0	13.0
18	1,4-diazobicyclo[2.2.2]octane	11.8	-0.5	12.3
	Heteroatom Neighbours			
20	Dioxane	11.4	-0.4	11.8
21	Dimethyl sulfoxide	15.7	3.8	11.9
22	Benzaldehyde†	12.6	-0.3	12.9
23	Hexamethylphosphoramide	12.1	-2.3	14.4
24	Diethyl ether	7.6	-3.8	11.4
	Allylic/Benzylic			
25	1,4-cyclohexadiene	12.0	-1.0	13.0
26	Toluene	14.7	0.9	13.7
29	Cumene	11.4	-1.9	13.3
30	Diphenylmethane†	13.6	-1.0	14.5
32	9,10-dihydroanthracene†	11.4	-3.2	14.6

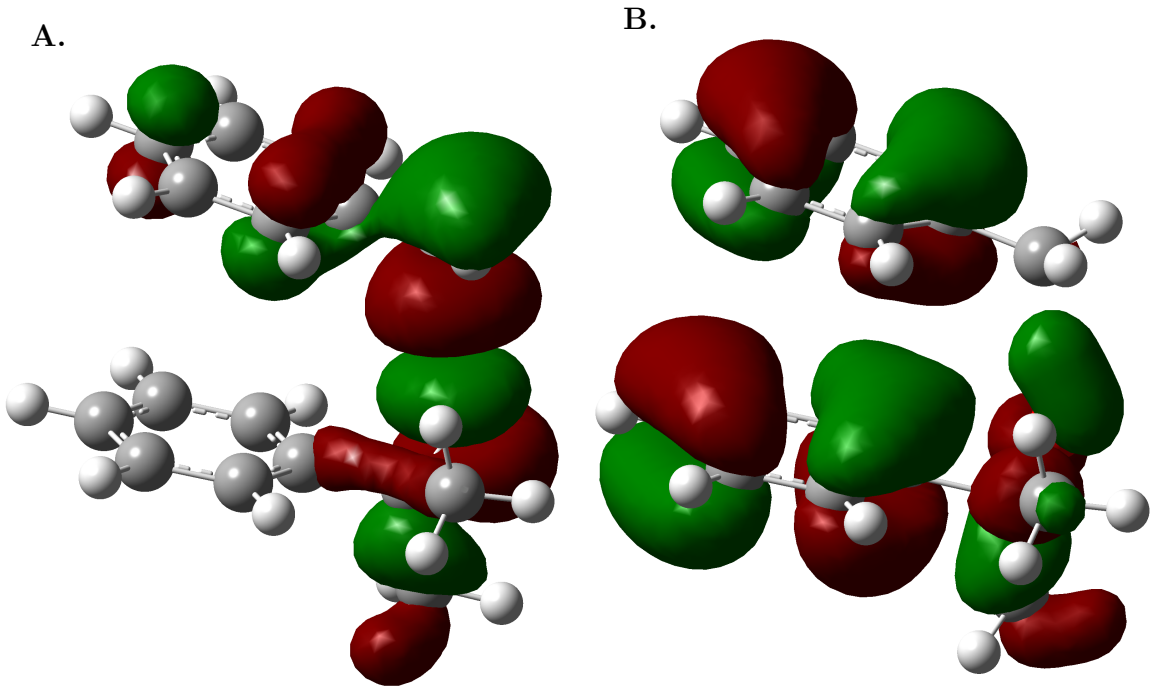

Figure 4.8: Structures of TS for HAT between CumO$^{\bullet}$ and toluene with **A.** SOMO and **B.** HOMO. The elements are coloured as grey for carbon, white for hydrogen, and red for oxygen.

For all of the TS structures of the reactions in Table 4.2, a conformation that maximizes non-covalent interactions while minimizing steric repulsion is adopted. In the cases of acetone, acetonitrile, hexamethylphosphoramide (HMPA), and DMSO, a very weak hydrogen bonding interaction is formed between the X=O (or C≡N for acetonitrile) moieties and the C-H of the methyl of CumO$^{\bullet}$. In all but two cases, this involves a cisoid (partially-stacked) complex so that dispersion interactions are maximized. The two outliers are benzaldehyde and cyclooctane. In order for benzaldehyde to adopt a cisoid TS structure, there are two possibilities. First, a T-shaped conformation could be adopted, rather than a slipped-parallel π-stacked conformation. On the basis of the benzene-benzene non-covalently bound dimer,[186] this conformation is very slightly favourable by circa 0.1 kcal mol^{-1}. However, this would require a rotation of nearly 90° of the C(CH$_3$)$_2$O$^{\bullet}$ of CumO$^{\bullet}$, which has an energetic cost[vii] of 4.3 kcal mol^{-1}, and so this conformation is unlikely. On the other hand, the C(CH$_3$)$_2$O$^{\bullet}$ of CumO$^{\bullet}$ could rotate to accommodate a partially slipped-parallel π-stacking conformation in the TS complex. Note that I was unable to obtain TS structures for either of the described possible cisoid conformations for the benzaldehyde-CumO$^{\bullet}$ TS complex, as geometry optimization calculations did not converge. For cyclooctane, the difference in free energy between the cisoid and transoid TS structures is 1.8 kcal mol^{-1}, however both structures were unable to be fully optimized and contain a secondary small imaginary frequency. The reason for the transoid TS structure being more stable is somewhat unclear, but it is possible that the non-optimal nature of the TS structures is the cause. Furthermore, it is possible that the cyclooctane

molecule undergoes a conformational change in forming the TS complex which was not accounted for in these calculations. Cyclooctane has many conformations that are close in relative energy.[187]

TS complex structures and mechanism aside, there is one striking feature in the reaction barriers calculated for HAT reactions involving CumO$^\bullet$: all the the reactions studied are entropy-controlled at 298 K. This means that the free-energy barrier, and thus rate constant, is controlled by the entropic contributions, rather than the enthalpic contributions, i.e., $-T\Delta S^\ddagger > \Delta H^\ddagger$. From the results in Table 4.2, it can be said that $-T\Delta S^\ddagger >> \Delta H^\ddagger$ for hydrogen abstraction by CumO$^\bullet$. One interpretation of these results is that CumO$^\bullet$ is so highly reactive that HAT is governed by trajectory, orientation, and degrees of freedom, factors that are normally associated with the A-factor in Arrhenius theory. In fact, in many cases, $\Delta H^\ddagger$ is calculated to be negative with respect to the separated reactants. This implies that a pre-reaction complex is formed, which, as was demonstrated in Chapter 3, can have significance on HAT reactivity with respect to the magnitude of the A-factor. Pre-reaction complex structures were not calculated in this work, however in some cases the systems have been studied in combined experimental and theoretical work. Some examples of previously calculated CumO$^\bullet$ + substrate pre-reaction complex binding enthalpies are: HMPA[viii] $\Delta H \approx$ -6 kcal mol^{-1}, DMSO $\Delta H \approx$ -5 kcal mol^{-1}, and 1,4-diazobicyclo[2.2.2]octane (DABCO)[37] $\Delta H \approx$ -0.1 kcal mol^{-1}. Note that the calculated enthalpic barrier herein is -0.5 kcal mol^{-1} for DABCO, a result that can be ascribed to differences in computational methods. In Ref.

[vii] Calculated at the LC-ωPBE-D3(BJ)/6-311+G(2d,2p) level of theory.

37, no dispersion correction was used, thus accounting for a less stable TS complex and pre-reaction complex. The calculated difference in enthalpy from pre-reaction complex to TS complex for DABCO was found to be only 1.0 kcal mol^{-1}.

The fact that hydrogen abstraction by $CumO^{\bullet}$ is entropy-controlled is perhaps unsurprising, given the work of Finn et al.[36], which demonstrated that HAT reactions involving various organic substrates and the closely related radical $t-BuO^{\bullet}$ are also entropy-controlled at room temperature. Furthermore, it has been shown that $CumO^{\bullet}$ and $t-BuO^{\bullet}$ display very similar hydrogen atom abstraction reactivities.[129,189–191] It is surprising then that these radicals remain so often applied as proxies for reactive oxygen species in kinetic studies. Future work should use extreme caution in applying $CumO^{\bullet}$ and $t-BuO^{\bullet}$ as chemical probes, as been noted in the past.[36,37,129] Note also that it is uncommon to encounter entropy-controlled reactions in organic chemistry, and they are often associated with non-Arrhenius behaviour. Other examples of reported entropy-controlled reactions include the addition of a carbene across a multiple bond,[192,193] and radical-radical recombination reactions.[194]

Classical physical organic chemical literature can explain why the reactions which are entropy-controlled do not follow "normal" LFERs.[195] Blackadder and Hinshelwood[196] defined three classifications for different types of LFERs, the first of which applies to the BEP principle: A series of reactions with constant entropy are controlled by enthalpy changes that are based on

[viii] DMSO and HMPA were studied in Ref. 133 at the B3LYP-DCP[188]/6-31+G(2d,2p) level of theory

electronic effects that do not affect the form of the TS. Therefore, reaction rates that involve non-isoentropic TS complex formation will not correlate with bond strengths, as is observed herein. It seems prudent at this point to suggest that expecting reactions to be isoentropic with respect to transition state formation is an over-simplification, especially given the number of factors that contribute to entropy in solvent phase chemistry.

4.6 Is the Bell-Evans-Polanyi principle valid?

The question still remains whether the BEP principle is valid or not. Recall from Equation 2.93 that E_a is related directly to $\Delta H^{\ddagger}$. Thus, if the BEP principle still holds for HAT reactions between CumO$^{\bullet}$ and organic substrates, then the calculated values of $\Delta H^{\ddagger}$ should be a function of C−H BDE. These data are plotted in Figure 4.9.

Perhaps unsurprisingly at this point, there is once again a great deal of scatter in the data. The cyclic alkanes fit into a linear relationship with perfect correlation (R^2=1.00). However, all other chemical groupings show almost no correlation. Therefore, the correlation seen for the cycloalkanes is an adventitious example of the BEP principle showing a linear relation between $\Delta H^{\ddagger}$ and BDE. Even the substrates with allylic/benzylic C−H bonds show only weak correlation in a BEP relation, although the experimental results show a reasonable correlation between $\log(k_H/n)$ and calculated BDEs. Therefore, the experimental results are likely serendipitous, especially considering the reactions are entropy-controlled and non-isoentropic.

Further analysis of the allylic/benzylic relation demonstrates a clear

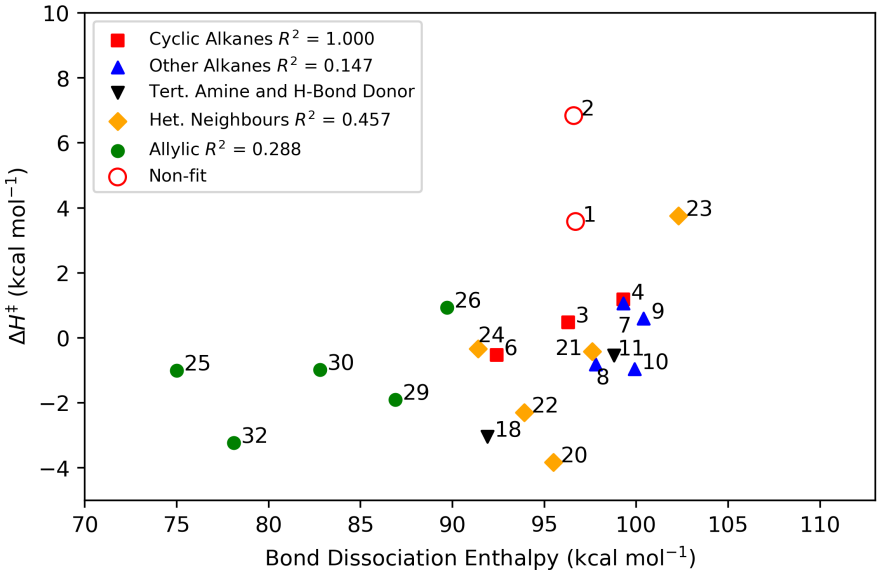

1	Acetone	2	Acetonitrile
3	Cyclopentane	4	Cyclohexane
6	Cyclooctane	7	2,2-dimethylbutane
8	2,3-dimethylbutane	9	Adamantane (2°)
10	Adamantane (3°)	11	Diethyl amine
18	1,4-diazobicyclo[2.2.2]octane	20	Dioxane
21	Dimethyl sulfoxide	22	Benzaldehyde
23	Hexamethylphosphoramide	24	Diethyl ether
25	1,4-cyclohexadiene	26	Toluene
29	Cumene	30	Diphenylmethane
32	9,10-dihydroanthracene		

Figure 4.9: Bell-Evans-Polanyi plot of calculated enthalpic barriers for HAT between CumO$^{\bullet}$ and substrates against BDEs calculated using the ROCBS-QB3 method.

breakdown in the BEP principle. If one begins with toluene with a BDE of 89.7 kcal mol^{-1}and $\Delta H^{\ddagger}$ of 0.9 kcal mol^{-1}, then the addition of two methyl substituents forms cumene, with a BDE of 86.9 kcal mol^{-1}and $\Delta H^{\ddagger}$ of -1.9 kcal mol^{-1}, indicating the stabilization of the TS by substituents. However, if one adds another phenyl group instead of two methyl groups, diphenylmethane is obtained, which has a BDE of 82.8 kcal mol^{-1}. This indicates that phenyl is a better radical stabilizing group, however $\Delta H^{\ddagger}$ is -1.0 kcal mol^{-1}, which is higher than that of cumene. The difference can be partially attributed then to differences in progress along the reaction coordinate. Evidence of this difference is the spin density localized on the O-centre of CumO$^{\bullet}$ in the TS complex, which should go to zero as the reactants move to products. The O$^{\bullet}$ spin densities are 0.533 e^{-}, 0.589 e^{-}, and 0.600 e^{-} for toluene, cumene, and diphenylmethane, respectively. Therefore, the progress along the reaction coordinate is furthest for toluene, and progressively less far for cumene and diphenylmethane. Note, however, that the O$^{\bullet}$ spin densities for cyclopentane, cyclohexane, and cyclooctane are 0.461 e^{-}, 0.425 e^{-}, and 0.420 e^{-}, respectively. Therefore the progress along the reaction coordinate for the cycloalkanes is not the same, even though the enthalpic barriers do correlate with BDE.

Such contradictory data makes it very difficult to draw any conclusions. Instead, I shall make some suggestions as to why the BEP principle is an incomplete theoretical construct for studying HAT reaction of CumO$^{\bullet}$ with organic substrates:

1. HAT reactions between CumO$^{\bullet}$ and these organic substrates may be

decidedly exothermic, resulting in reactions with no enthalpic barrier associated with the breaking of a C−H bonds and the formation of an O−H bond. This is supported by the fact that the calculated enthalpic barriers are all very low or even negative. Therefore, any remaining nominal activation energy is a result of stereo-electronic interactions between $CumO^{\bullet}$ and the substrate. Also, the high reactivity of $CumO^{\bullet}$ also suggests that abstraction from the weakest bond in a substrate will not always occur. The site of abstraction will most likely be determined by the orientation of the substrate upon collision. This is likely an additional reason why $\log k_H/n$ does not correlate with the calculated C−H BDEs.

2. Polar effects have been shown to be extremely important in the stability of the TS complex.[197] The species involved in HAT reactions are often neutral radicals, thus the influence of charge transfer in the TS complex can have important implications. Consider the TS of a generic HAT reaction in Scheme 4.3, there are four obvious resonance forms. Oxygen-centred radicals are electrophilic in nature, thus the importance of the third resonance structure increases. The BEP principle does not account for polarity in the TS complex, as these effects are not captured by the BDE of the substrate, thus $\Delta H^{\ddagger}$ does not correlate well with BDE. This issue was addressed by Roberts and Steel[198], who suggested an extension of the BEP principle to include simple empirical parameters that capture the polar effects in the transition state.

$$\left[\mathrm{X\text{–}H\text{–}Y}\right]^{\ddagger}$$

$$[\mathrm{X^{\bullet}H{-}Y}]^{\ddagger} \longleftrightarrow [\mathrm{X{-}HY^{\bullet}}]^{\ddagger} \longleftrightarrow [\mathrm{X{:}^{-}H^{\bullet}Y^{+}}]^{\ddagger} \longleftrightarrow [\mathrm{X^{+}H^{\bullet}Y{:}^{-}}]^{\ddagger}$$

Scheme 4.3: A generic HAT transition state structures and possible resonance forms.

3. The BEP principle is an over-simplification that does not capture nearly enough of the physics associated with the deceptively complex hydrogen abstraction reactivity of $\mathrm{CumO^{\bullet}}$ (or $t{-}\mathrm{BuO^{\bullet}}$). Therefore, I suggest that the BEP principle should not be used as a tool for predicting activation energies or rate constants. One method that has been popularized by Mayer is the use of Marcus cross-relations.[29] This predictive method has also been used to explain reactions that have negative enthalpic barriers.[118] An alternative approach is that of Zavitsas, that predicts activation energies based on so-called "triplet repulsion"[ix] and radical delocalization.[199,200] It is clear from the analysis herein that the BEP principle is valid only as a conceptual framework, rather than a true linear relationship.

[ix] Zavitsas uses the term "triplet repulsion" to describe repulsion between the parallel spins of the hydrogen atom acceptor and donor atoms (↑↓↑ or ↓↑↓) in the TS complex.

Appendix B

Chapter 4 Additional Data

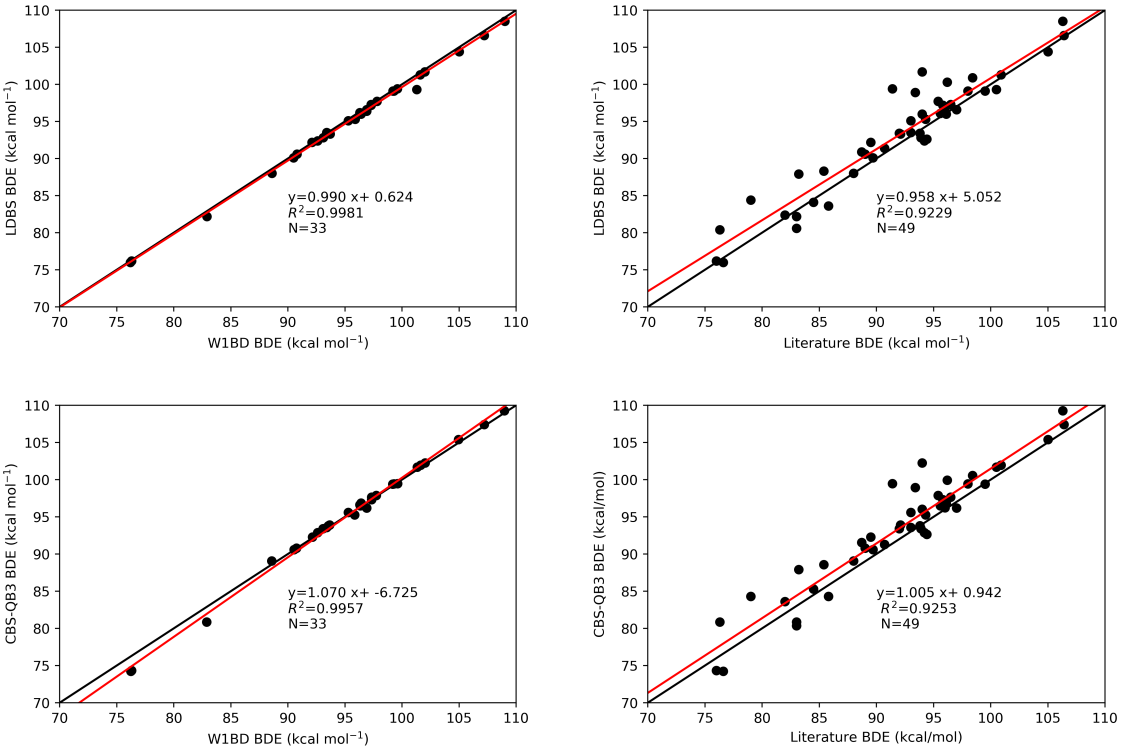

Figure B.1: One-to-one plots of composite methods compared to literature and W1BD.

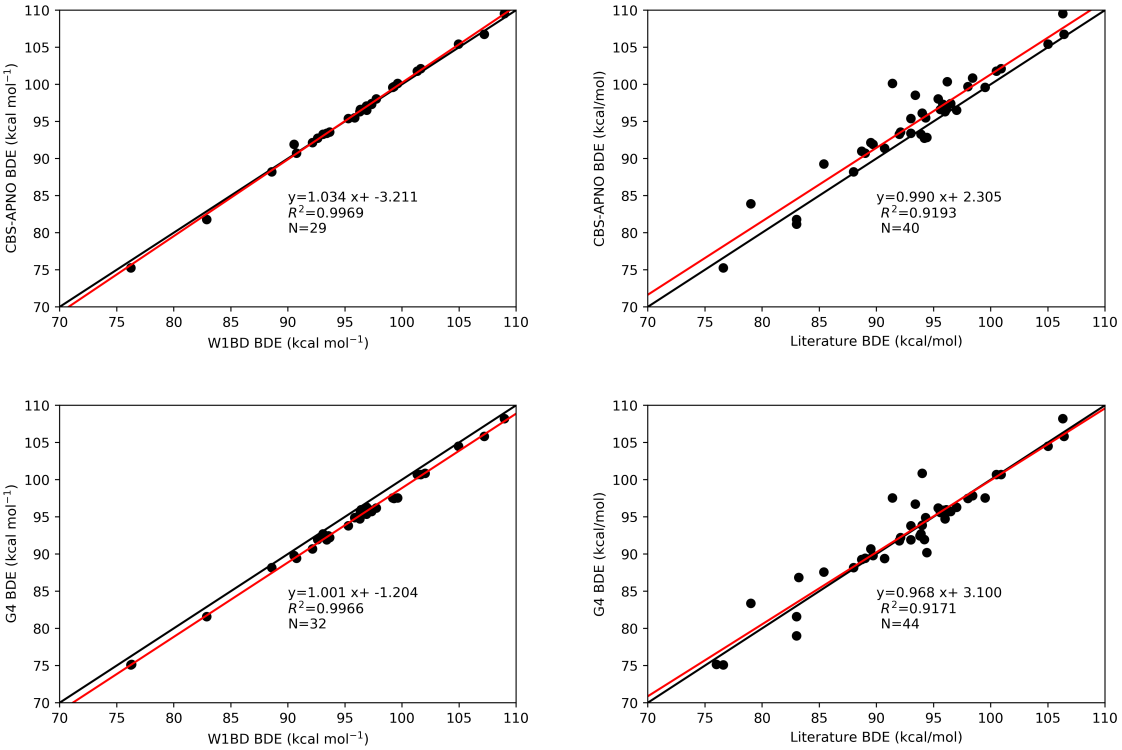

Figure B.1: Continued: One-to-one plots of composite methods compared to literature and W1BD.

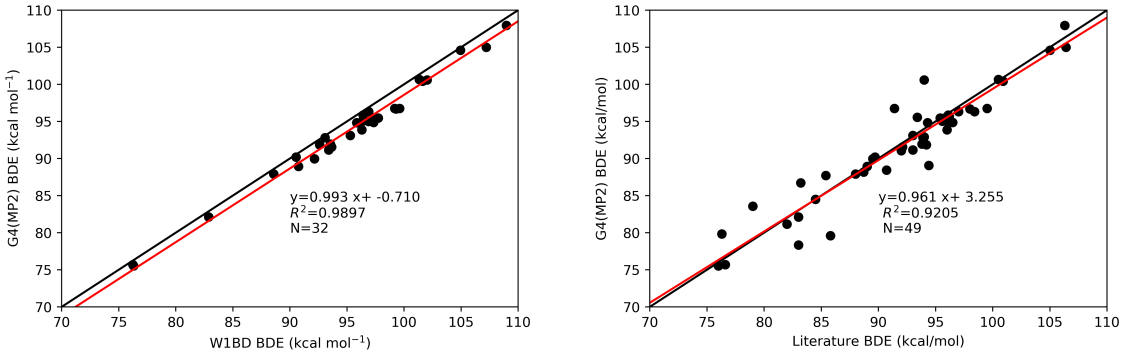

Figure B.1: Continued: One-to-one plots of composite methods compared to literature and W1BD.

Table B.1: Summary of experimental rate constants ($M^{-1}s^{-1}$) and literature[167] bond dissociation enthalpies (BDEs, kcal mol^{-1}).

Molecule	k_H	Normalized k_H	BDE
1,4-cyclohexadiene	6.60×10^7	1.65×10^7	76
1,4-diazabicyclo-[2.2.2]octane	9.60×10^6	8.00×10^5	93.4
2,2-dimethylbutane	9.50×10^4	4.75×10^4	98
2,3-dimethylbutane	5.60×10^5	2.80×10^5	95.4
9,10-dihydroanthracene	5.04×10^7	1.26×10^7	76.3
Acetone	$< 1 \times 10^4$	2×10^3	96

Acetonitrile	$< 1\times10^{4}$	3×10^{3}	97
Adamantane (2°)	6.90×10^{6}	5.75×10^{5}	98.4
Adamantane (3°)	6.90×10^{6}	1.73×10^{6}	96.2
Benzaldehyde	1.20×10^{7}	1.20×10^{7}	88.7
Benzyl alcohol	2.97×10^{6}	1.49×10^{6}	79
Cumene	5.60×10^{5}	5.60×10^{5}	83.2
Cycloheptane	2.20×10^{6}	1.57×10^{5}	94
Cyclohexane	1.10×10^{6}	9.17×10^{4}	99.5
Cyclooctane	2.98×10^{6}	1.86×10^{5}	94.4
Cyclopentane	9.54×10^{6}	9.54×10^{5}	95.6
Dibenzyl ether	5.60×10^{6}	1.40×10^{6}	85.8
Diethyl ether	2.60×10^{6}	6.50×10^{5}	93
Dimethyl sulfoxide	1.80×10^{4}	6.00×10^{3}	94
Dioxane	8.20×10^{5}	1.03×10^{5}	96.5
Diphenylmethane	8.71×10^{5}	4.36×10^{5}	84.5
Ethylbenzene	7.90×10^{5}	3.95×10^{5}	85.4
Hexamethylphorsphoramide	1.87×10^{7}	1.04×10^{6}	
Morpholine	5.00×10^{7}	1.25×10^{7}	92
Piperazine	2.30×10^{8}	2.90×10^{7}	93
Piperidine	1.10×10^{8}	2.80×10^{7}	89.5
Pyrrolidine	1.20×10^{8}	3.10×10^{7}	89

Tetrahydrofuran	5.80×10^6	1.45×10^6	92.1
Toluene	1.85×10^5	6.17×10^4	89.7
Triethylamine	2.10×10^8	3.5×10^7	90.7
Triphenylmethane	3.04×10^5	3.04×10^5	81